Microfluid Nanofluid (2013) 15:161–172
DOI 10.1007/s10404-013-1138-4

RESEARCH PAPER

Highly sensitive identification of foodborne pathogenic *Listeria monocytogenes* using single-phase continuous-flow nested PCR microfluidics with on-line fluorescence detection

Bowen Shu · Chunsun Zhang · Da Xing

Received: 30 August 2012 / Accepted: 8 January 2013 / Published online: 25 January 2013

Abstract Highly sensitive detection of foodborne pathogens such as *Listeria monocytogenes* (*L. monocytogenes*) is crucial to the prevention and recognition of problems related to public health and legal repercussions, due to "zero tolerance" standard adopted for food safety in many countries. Here we first propose a single-phase continuous-flow nested polymerase chain reaction (SP-CF-NPCR) strategy for identification of the low level of *L. monocytogenes* on an integrated microfluidic platform. The PCR reactor is constructed by a disposable capillary embedded in the grooved heating column, coupled with a fluorescence microscopy for on-line semi-quantitative end-point fluorescence detection. As a proof-of-concept microfluidic system, the nested PCR is performed in a continuous-flow format without the need of any non-aqueous oil or solvent. On this device, the performance of nested PCR amplification has been evaluated by investigating the effect of reaction parameters, including polymerase concentration, flow rates, and template DNA concentration. In addition, the types of samples the presented system can accept, such as the unpurified DNA samples and artificially contaminated clinical stool samples were also evaluated. With the optimized reaction parameters, 0.2 copies/μL of genomic DNA from *L. monocytogenes* can be detected on the presented device. To our knowledge, this is the highest detection sensitivity in single-phase continuous-flow PCR microsystems reported so far. The high sensitivity of the analysis method, combined with the flexibility of reaction volumes and convenience of continuous operation, renders it to be further developed for potential analytical and diagnostic applications.

Keywords Continuous-flow nested PCR · Single-phase · Microfluidics · Online fluorescence detection · *Listeria monocytogenes*

1 Introduction

A worldwide increase in the incidence of foodborne illness has resulted in significant economic and public health impact. Current standards for pathogen detection and identification mainly rely on the labor-intensive and lengthy culturing techniques, as it takes 2–3 days for initial results, and up to 7–10 days for confirmation (Park et al. 2011). Furthermore, presently in many countries such as United States, China, and most of European countries, there is a zero tolerance policy that mandates that no viable pathogens are allowed in certain foods (Batt 2007). Therefore, the development of fast and sensitive detection approaches enabling the identification of low levels of the foodborne pathogens is necessary.

Polymerase chain reaction-based genetic analysis, as a gold standard method for the identification of pathogenic bacteria, incorporates with microfluidic platform to take full advantages of low sample and reagent consumption, rapidness, portability and integration, which makes microfluidic PCR the promising candidate for rapid and sensitive detection of foodborne pathogens (Liu et al. 2009;

Electronic supplementary material The online version of this article (doi:10.1007/s10404-013-1138-4) contains supplementary material, which is available to authorized users.

B. Shu · C. Zhang (✉) · D. Xing (✉)
MOE Key Laboratory of Laser Life Science and Institute of Laser Life Science, College of Biophotonics, South China Normal University, Guangzhou 510631, China
e-mail: zhangcs@scnu.edu.cn; zhangcs_scnu@126.com

D. Xing
e-mail: xingda@scnu.edu.cn

Ramalingam et al. 2009, 2010). During the past years, efforts for high sensitivity of microfluidic PCR assay have proceeded along two fundamental tracks: optimizing sample pre-processing for obtaining high PCR efficiency and high concentration of target analytes, and improving the method and instrument of post-PCR analysis. To these ends, different technologies/methods have been adopted by single-phase microfluidic PCR devices and the two-phase microfluidic ones.

For single-phase microfluidic PCR, a single aqueous phase containing PCR components is used to fill the chamber or channel in static microfluidic (Northrup et al. 1993; Yang et al. 2002; Cady et al. 2005) and dynamic continuous-flow (Kopp et al. 1998; Chen et al. 2004; Njoroge et al. 2011; Pjescic and Crews 2012) PCR devices, which not only provides the convenience for functional integration of DNA purification and concentration with microfluidic PCR module, but also pave ways to developing alternative techniques for highly sensitive post-PCR analysis including capillary electrophoresis (CE) and microarrays (Liu et al. 2004; Beyor et al. 2009; Qiu et al. 2011; Manage et al. 2011; Njoroge et al. 2011; Pjescic and Crews 2012). For example, Beyor et al. presented a single-phase stationary chip system that integrated cell preconcentration, purification, PCR, and CE analysis with a detection limit of 0.2 CFU/μL for *Escherichia coli* O157 (Beyor et al. 2009). Recently, a flow-through microfluidic chip capable of performing on-chip lysing, PCR, and spatial DNA melting analysis for one-step genetic detection from raw saliva samples was demonstrated by Pjescic and Crews (2012). In comparison with static PCR systems, continuous-flow PCR systems have the remarkable advantage of rapid cycling speed. However, they often suffer from some problems: the PCR inhibition, due to the interaction between the PCR mixture and the reactor substrate, is more evident in a continuous-flow format (Polini et al. 2010; Hua et al. 2010), and axial dispersion caused by the parabolic velocity profile of the channel flow-field can lead to dilution of samples. These factors may explain why most of single-phase continuous-flow microfluidic PCR devices have relatively low detection sensitivity.

Within the two-phase microfluidic PCR devices, a non-aqueous phase is used to confine the reaction mixture for performing PCR amplification. When the second phase (oil or solvent) is used, the evaporation loss of reaction samples can be reduced; non-specific surface adsorption can be mitigated. These features enable two-phase microfluidic PCR devices to carry out high-efficient PCR in reduced reaction volumes, which allows for the possibility of increased throughput and sensitivity. Recently, several droplet-based PCR microsystems have been successfully developed with high sensitivity of detection at a single copy of nucleic acid molecule or at a single cell level (Zhang and Xing 2010; Hua et al. 2010; Zeng et al. 2010; Shi et al. 2011). The increased sensitivity mainly benefits from the combination of two approaches, one is to increase relative analyte concentration by compartmentalizing target DNA samples to small volumes in the range of nanoliters or even femtoliters, and the other is to alleviate non-specific surface adsorption by dispersing aqueous droplets into an immiscible oil phase. However, in the field of foodborne pathogen detection, this two-phase microdroplet technology may possess some challenges. First, pathogens in foods are often present at such a low level that the analysis in a relative large PCR volume (ranging from 10 to 100 μL or even higher) is desirable (Yang et al. 2002; Qiu et al. 2010; Park et al. 2011; Ritzi-Lehnert et al. 2011). On one hand, the volume below microliter-scale would be problematic for statistically containing enough of the target molecules to ensure confidence in the result of the single assay (Yang et al. 2002). On the other hand, only one of several million picoliter-scale droplets will contain one copy of the target molecule in high-throughput assay without regard to the non-uniform encapsulation of the microdroplets (Wang and Burns 2009). Secondly, multistep or downstream processes (e.g., restriction digestion, and hybridization) of droplets is not easy-to-operate due to the confines of the immiscible phase (Wang and Burns 2009; Schaerli and Hollfelder 2009; Zhang and Xing 2010).

As an alternative strategy to improve the sensitivity of PCR assay, nested PCR is developed to overcome the common obstacle of standard PCR protocol, where low levels of starting molecules often fail to be amplified to a detectable level due to the competition between the desired fragments and non-specific products by increasing the number of cycles. Up to now, several nested PCR microfluidic systems have been well developed (Anderson et al. 2000; Wang and Burns 2010; Ritzi-Lehnert et al. 2011; Sun et al. 2011a, b; Sciancalepore et al. 2011; Lok et al. 2012). Early in 2000, Anderson et al. (2000) reported the first nested PCR microfluidic device, which was capable of detecting as few as 300 copies of RNA from HIV serum samples. In recent years, Wang and Burns (2010) presented a static droplet-based nested TaqMan® PCR platform with a detection limit of $\sim 6.69 \times 10^2$ copies/μL of λ-DNA. Ritzi-Lehnert's group presented a sample-in-answer-out microfluidic system capable of performing the nested multiplex reverse-transcript (RT)-PCR in <1 h at a high volume of 120 μL (Ritzi-Lehnert et al. 2011). Sun et al. (2011a, b) developed a chamber-based PCR microchip combining RNA RT reaction in the liquid phase and nested PCR amplification on the solid phase for fast screening of avian influenza virus by DNA microarray integrated on the chip. Sciancalepore et al. (2011) demonstrated the first nested PCR for rapid detection of tyrosinase gene on an oscillatory-flow droplet-based microfluidic device, where

10^3 copies of tyrosinase transcript in 1-μL droplet could be amplified in 47 min. Lok et al. (2012) have recently introduced the nested PCR protocol into a magnetically actuated circular closed-loop PCR microsystem and obtained 80 % success in detecting a single copy of λ-DNA in a total volume of 5 μL. These works demonstrate that the microfluidic nested PCR has the great potential for performing rapid and highly sensitive nucleic acid detection. Within the nested PCR microfluidic devices reported so far, however, the single-phase continuous-flow nested PCR (SP-CF-NPCR), which cannot only overcome the disadvantage of low detection sensitivity associated with conventional single-phase continuous-flow PCR, but also circumvent some shortcomings of two-phase droplet PCR microfluidics, has not been presented.

In this study, we first report a SP-CF-NPCR microfluidics for highly sensitive detection of foodborne pathogens. The reaction mixture continuously flowed through three isothermal zones of a cylindrical helical-channel microfluidic device, where the complete nested PCR protocol (first and second PCR run) was carried out, to detect the foodborne pathogenic *L. monocytogenes* (Fig. 1a). The disposable polytetrafluorethylene (PTFE) tube reactor not only enables a more convenient sample handing, but also can be easily replaced with a new tubing to prevent samples cross-contamination. On the presented microfluidics, the effect of some reaction parameters on the performance of SP-CF-NPCR has been investigated, including polymerase concentration, flow rate, and template DNA concentration. In addition, the on-line fluorescence detection system is used to provide rapid detection of nested PCR product. The results show that the minute amount of genomic DNA from *L. monocytogenes* can be successful amplified and detected in a short time.

2 Materials and methods

2.1 Description of the continuous-flow PCR microfluidic device

The cylindrical helical-channel CF-PCR device integrated with the on-line fluorescence detection consists of four main components (Fig. 1b): (1) the computer-controlled, LabVIEW-based temperature measurement and control system, which was developed in our laboratory (Zhang and Xing 2009); (2) the continuous-flow microfluidic PCR system including a disposable PTFE capillary tube, three copper heating columns, three resistance cartridge heaters, three K-type thermocouple sensors; (3) the programmable precision syringe pump (KDS210, KD Scientific Inc., Holliston, MA, USA) for fluid actuation; (4) the on-line fluorescence detection system that comprises the M17 fluorescence microscope (Bio-rad, Hercules, USA) and the computer controlled, cooled charge-coupled device (CCD) camera (MC15, Guangzhou Ming-Mei technology, Guangzhou, China) for product analysis. The transparent commercial PTFE tube (0.5 × 0.9 mm [o.d. × i.d.], Wuxi Xiangjian tetrafluoroethylene Product, Wuxi, China) was wrapped around the helical machined grooves (1.1 × 1.1 mm [width × depth]) on the surface of a heating column to form a 30-turn helix, thus corresponding to 30 PCR cycles. The copper column (35 × 18 × 70 mm [o.d. × i.d. × height]), which was fabricated by the Automation Engineering R&M Centre (AERMC, Guangdong Academy of Sciences, Guangzhou, China), was segmented into three heating zones, with the extension one being twice the size of the other two, to provide the denaturing, annealing and extension phase of the PCR. For obtaining a better temperature control and the compact structure of the thermal cycler, the annealing zone was cooled by circulating water to maintain at the necessary temperature. The two ends of copper column were clamped by the bakelite brackets with an air gap of ~7 mm between the three segments to further eliminate temperature cross-talk. Each zone was covered with a thin layer of cooper foil, which was encapsulated by a foam insulation tape to eliminate convective heat loss from each thermal zone, thus minimizing the temperature gradient in the capillary tube. A heater cartridge (6 × 70 mm [o.d. × height], 100 W, Guangzhou Haoyi Thermal Electrics Factory, Guangzhou, China) and a K-type thermocouple (0.005-inch diameter, Omega Engineer, Stamford, CT, USA) were fixed into each segment. The temperature signals from the thermocouple through a TBX-68T terminal block (National Instruments) were acquired using the analog input of a PCI-4351(National Instruments) card and converted to digital ones as the feedback signals for the homemade fuzzy proportional/integral/derivative (PID) control algorithm that was programmed with LabVIEW (version 2010, National Instruments).

2.2 Reagents and samples

DNA template for SP-CF-NPCR was isolated from *L. monocytogenes* CMCC54007 (Guangzhou Institute of Microbiology, Guangzhou, China) using the TIAMamp Bacterial Genomic DNA Extraction Kit (Tiangen Biotech Co., Ltd. Beijing, China) according to the manufacturer's instruction. The isolated DNAs were quantified on the Eppendorf BioPhotometer with a concentration of 135 ng/μL or 4.18×10^7 copies/μL. The outer-primers were designed for amplification of the 430-bp product of the LLO-encoding gene (hlyA, accession numbers AF253320) from *L. monocytogenes*, while the inner-primers were designed to a 227-bp region of the targeted 430-bp first-run PCR product in the second-run PCR amplification. All oligonucleotide primers (Table 1), which were designed with Primer

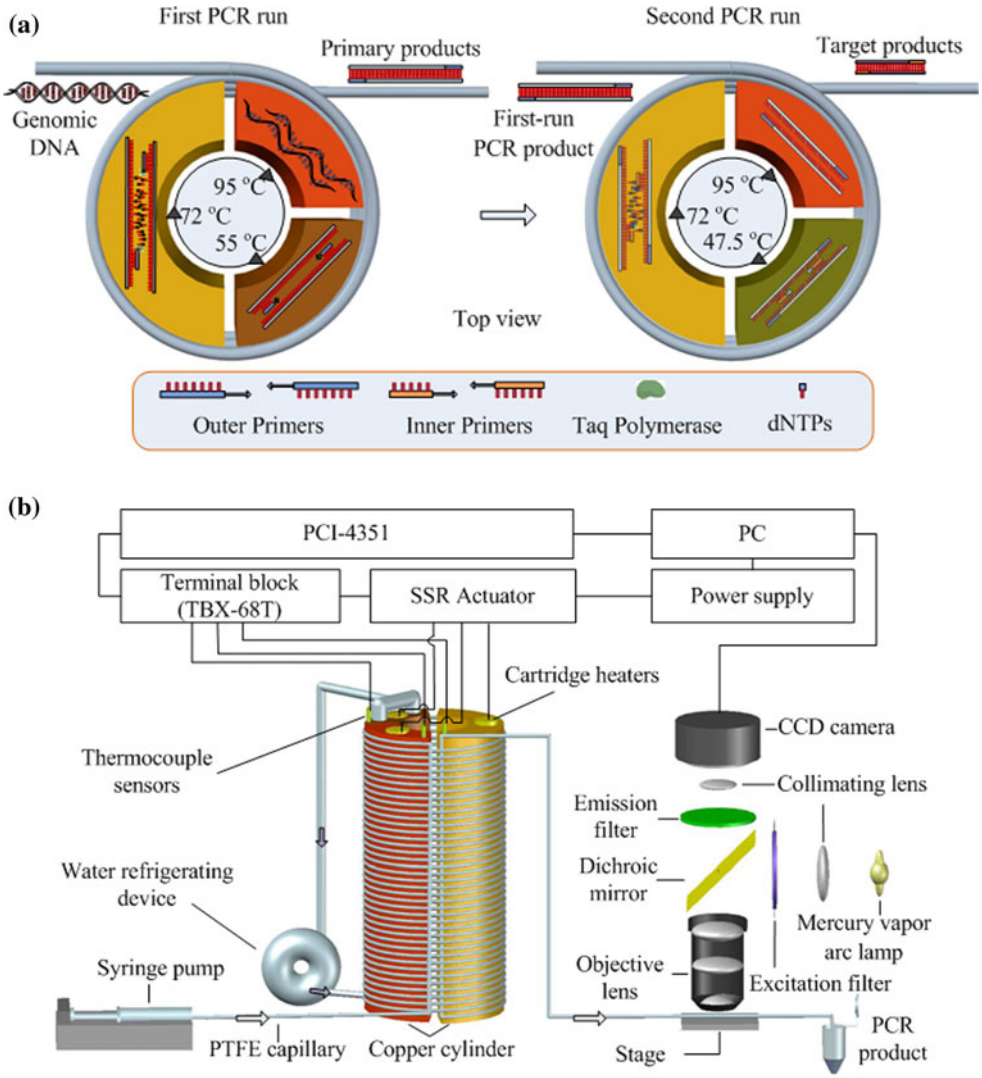

Fig. 1 Schematic of the single-phase continuous-flow nested PCR (SP-CF-NPCR) (**a**) and schematic diagram of the cylindrical helical-channel continuous-flow nested PCR microfluidics with on-line fluorescence detection (**b**)

Premier (version 6, PREMIER Biosoft, USA), were synthesized by Invitrogen Biotechnology Co., Ltd. Chemicals for PCR mixtures, including 10 × PCR Buffer (Mg^{2+} Plus), deoxynucleotide triphosphate (dNTP) mixture and Taq polymerase, were purchased from TaKaRa Biotechnology (Dalian) Co., Ltd. Bovine serum albumin (BSA, Fraction V, Purity ≥98 %, Biotechnology Grade, cat.no.735094) was bought from Roche Diagnostics GmbH (Mannheim, Germany). GoldView™ and SYBR Green I dyes were obtained from SBS Genetech Co., Ltd. (Beijing, China). DS™ 2000 DNA markers, which contain 2,000, 1,000, 750, 500, 250, and 100 bp DNA fragments, were provided by Dongsheng Biotech Co., Ltd. (Guangzhou, China).

2.3 Capillary inner surface passivation

To reduce reaction inhibition and improve reaction efficiency, the PFTE capillary inner surface was cleaned and passivated according to the protocol of our previous work (Li et al. 2011a, b), with minor modifications. Briefly, the capillary tube was rinsed with DNA-free double distilled (dd) H_2O. Then, to further protect the reaction from surface inhibitory effect, both static and dynamic passivation using BSA as the blocking agent were applied for each PCR reaction. For the static passivation, a 10-μL 1× PCR buffer containing BSA [1 % BSA (w/v), 1 × PCR buffer, and 0.1 % Triton-100(v/v)] was introduced to the capillary before each reaction solution. For dynamic passivation, the addition of 0.04 % BSA (w/v) to the master mixture was used to render the inner surface PCR-compatible.

2.4 Nested-PCR protocol

Unless demonstrated otherwise, a 25-μL standard PCR mixture used in each PCR reaction consisted of 1× PCR buffer, 1.5 mM $MgCl_2$, 200 μM each dNTP, 1× SYBR Green I, 0.04 (w/v) BSA, 300 nM each of the primers, and 0.2 unit/μL of Taq polymerase and varied amounts of DNA

Table 1 Detailed information about the primers of nested PCR

Primer pairs		DNA sequences (5′–3′)	Position	T_m (°C)	Product size (bp)
Outer	Sense	AACATATCCAGGTGCTCTCGTAA	372	55.6	430
	Antisense	GGAAGGTCTTGTAGGTTCATTAACA	801	55.4	
Inner	Sense	AATCAACCAGATGTTCTC	418	44.2	227
	Antisense	GATTCACTGTAAGCCATT	644	44.6	

templates. The nested PCR cycling protocol in the capillary reactor was described as follows: for the first PCR run, 2 μL of the template DNA was added in 23 μL of PCR master mixture containing the outer-primers. Then, the flow rate of 2 mm/s was used to drive the reaction solution, corresponding to the residence times of 10 s in the denaturing zone (95 °C), 10 s in the annealing zone (55 °C), and 22 s in the extension zone (72 °C), respectively. After the first PCR run, 2 μL of the amplified DNA product was used as templates and was added to 23 μL PCR master mixture containing the inner-primers for the second PCR run. The second PCR run consisted of 6 s at 95 °C, 6 s at 47.5 °C, and 14 s at 72 °C, with flow rate at 3.5 mm/s. The total runtime of the nested PCR performed in the microfluidic device was about 41 min.

To characterize PCR performance on the microfluidic device, a similar nested PCR protocol was also conducted in a commercial MasterCycler gradient PCR machine (Eppendorf, Hamburg, Germany) as a positive control. For the first PCR run, the 25-μL PCR master mixture containing 2 μL of DNA samples were thermally cycled under the following conditions: 95 °C denaturation for 35 s, 30 cycles of 95 °C for 10 s, 55 °C for 10 s, 72 °C for 22 s, followed by a 35 s extension at 72 °C. For the second PCR run, 2-μL product of the first-run PCR was added into the PCR mixture and was amplified as such: 35 s at 95 °C, 30 cycles of 10 s at 95 °C, 10 s at 47.5 °C, 22 s at 72 °C, and 35 s at 72 °C. The total runtime for carrying out the nested PCR protocol in the thermal cycler was 73 min.

2.5 Analysis of products

The amplification products were directly analyzed in the reaction capillary using on-line fluorescence detection method. Briefly, the capillary was placed on a stage, the excitation light from a 100-W mercury vapor arc lamp (HBO, OSRAM, Munich, Germany) was filtered by a 450–490 nm bandpass excitation filter and laterally reflected at 90° by a 505-nm bandpass dichroic mirror and focused into the capillary through a 10× (0.25 NA) microscope objective (Bio-rad). The fluorescence was collected through the same objective and dichroic mirror, passed through a 520 nm emission filter and focused on a cooled CCD camera. The camera, which was connected to the computer with one USB cable, was used for acquiring sequential pictures of fluorescence in the capillary. The images were analyzed with MS 1.0 software (Guangzhou Ming-Mei technology) as described previously (Li et al. 2011a, b). After on-line fluorescence detection, 5 μL of the products with 1 μL 6× loading buffer were separated using agarose gel electrophoresis (AGE). The gel was prepared with 2.25 % (w/v) of agarose in 1× TAE buffer containing 0.5 μL/mL GoldView^{TM} dye. The gel was run for 30 min at 100 V, and then visualized under UV light. DNA band sizes were determined relative to the DS^{TM} 2000 DNA markers.

3 Results and discussion

3.1 Evaluation of the continuous-flow PCR reactor

Polymerase chain reaction is much temperature-sensitive, and over 1 °C of temperature variations can result in significant decrease of PCR efficiency. Thus, accurate and precise temperature control is crucial for an effective and reproducible PCR (Peham et al. 2011). In the presented microfluidic device, the contact head of thermocouple was sheathed in the PTFE tubing with a length equal to the depth of small hole that is near the exterior surface of each columnar block. Therefore, the temperature sensors nearly experience the equivalent thermal conditions to the liquid sample in the reaction tube, as can improve continuous-flow PCR temperature control. The capillary tube was embedded into the grooves on the heating copper block and its bottom was in direct contact with the copper surface. Then, each temperature zone was covered with a thin cooper foil, whose edges are in contact with a raised piece of the copper cylinder corresponding to that zone. The copper foil provides heating from above and improves temperature uniformity inside the reaction capillary tube. The thermal insulation provided by the bakelite brackets, air gaps between blocks, and foam insulator can further improve temperature uniformity across of the capillary over a heating block. In addition, a circulating water bath was used to refrigerate the annealing zone to obtain a steady and uniform annealing temperature. On the present device, the temperature values obtained at three

different locations of each heating zone (near each end and in the middle of the heating block) indicated that the temperature deviation in each temperature zone was smaller than 0.3 °C. Fig. S1a and b in the Electronic Supplementary Material (ESM) showed the temperature changed with time at three temperature control points of the presented device during a typical SP-CF NPCR experiment. The result demonstrated that the steady-state temperature overshoot and undershoot in each reaction zone were very small and the maximum standard deviation was 0.18 °C. Therefore, the temperature temporal stability and spatial uniformity on the presented microfluidic device is good, as is advantageous for obtaining an effective and reproducible nested PCR amplification. In addition, it is necessary to note that according to the work reported by Chen et al. (2005b), the time constants of the extension, denaturing and annealing zones within the presented device are estimated to be 8.2, 1.3, 1.3 s, and the time constant of the PTFE reaction tubing is approximately 0.4 s (Fig. S2). Therefore, the temperature response time of the heating process is dominated by the time constant of the copper-heating blocks.

3.2 Effect of polymerase concentration on single-phase continuous-flow nested PCR

Although the PTFE tubing is an ideal biocompatible material for PCR (Peham et al. 2011), adsorption of biomolecules, especially the Taq DNA polymerase, is a potential problem of SP-CF PCR microfluidics due to the high SVR of the long channel (Prakash et al. 2008). Therefore, it is necessary to evaluate the effect of polymerase on SP-CF-NPCR (Fig. 2; Fig. S3). It can be seen from Fig. 2 that a gradual increase in first-run PCR yield was observed when the amount of Taq DNA polymerase ranging from 0.05 to 0.15 unit/μL was employed. The first-run continuous-flow PCR yield obtained at 0.15 unit/μL of Taq polymerase concentration was higher than that of the conventional PCR in the case of 0.05 unit/μL. When the concentration of Taq DNA polymerase further increased to 0.2 or 0.25 unit/μL, however, the first-run PCR yield no longer raised obviously. As a result, the amount of Taq polymerase trends to saturate around 0.2 unit/μL. As seen in Fig. 2, the yields of the second-run PCR products showed a nearly linear increase when the amount of Taq DNA polymerase ranged from 0.05 to 0.25 unit/μL. The difference of the effect of polymerase concentration between first-run and second-run continuous-flow PCR is possibly due to the difference in amount and length of the DNA templates or the sequences of primers used in these two runs. It is necessary to note that if the Taq DNA polymerase of low concentrations were exploited (for example 0.05 and 0.1 unit/μL), the band of product could be obviously observed on the fluorescence and gel images ("0.05" and "0.1" columns in Fig. 2a; lanes 2 and 3 in

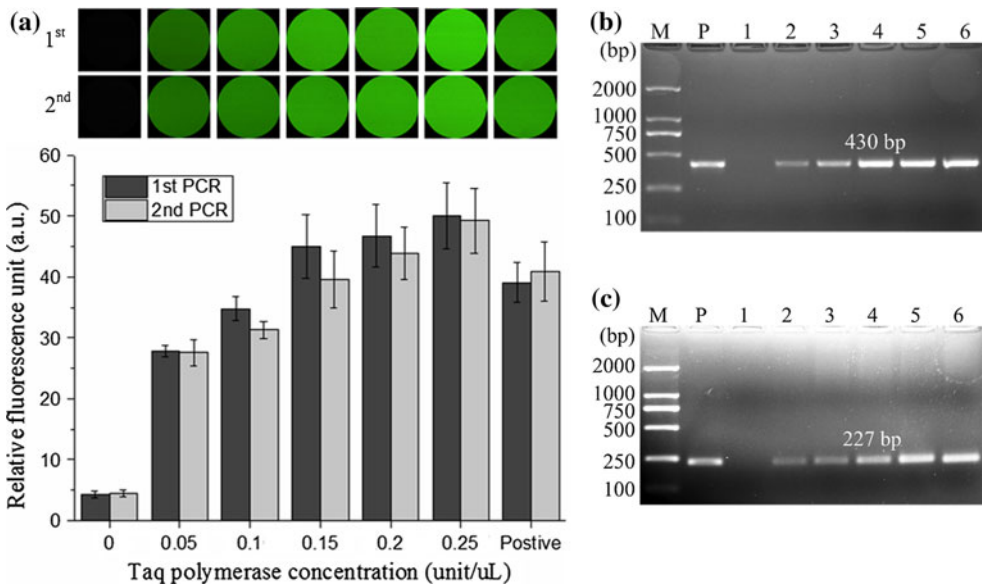

Fig. 2 Effect of polymerase concentration on SP-CF-NPCR. **a** Fluorescence detection of the SP-CF-NPCR products. Here, the *error bars* represent the standard deviation of the average values of three individual experiments. **b** Gel analysis of the first-run products. *Lane P* the positive control PCR product from the conventional PCR machine with 0.05 unit/μL Taq polymerase; *Lane 1–6* the first-run products from the SP-CF-NPCR with different concentrations of Taq polymerase (0, 0.05, 0.1, 0.15, 0.2, 0.25 unit/μL, respectively) using 2 μL DNA template of 2.5×10^5 copies/μL. **c** Gel analysis of the second-run products. *Lane P* the positive control PCR product from the conventional PCR machine with 0.05 unit/μL Taq polymerase. *Lane 1–6* the second-run products from the SP-CF-NPCR at the flow rate of 2 mm/s with different concentrations of Taq polymerase (0, 0.05, 0.1, 0.15, 0.2, 0.25 unit/μL, respectively). Here, 2-μL first-run PCR product that was diluted 400-fold with DNA-free water was used as second-run PCR templates

Fig. 2b, c), but the intensities of the fluorescence and gel results are weaker than those of the positive controls obtained on the conventional machine ("positive" column in Fig. 2a; lane P in Fig. 2b, c). This result implies that in the case of 0.05 or 0.1 unit/μL polymerase concentration small amount of polymerase remains in the PCR reaction mixture instead of completely being absorbed to the inner surface of the channel. This phenomenon may be attributed to the fact that the addition of BSA counteracts adsorption of Taq polymerase by competing for adsorption sites of inner surface (Crabtree et al. 2012).

3.3 Effect of flow rates on single-phase continuous-flow nested PCR

Pursuing fast PCR is one of the major motivations in the development of PCR microfluidics. The cycling rate of continuous-flow PCR depends, to some extent, on the flow velocity of the PCR solution, the material and size of the reaction channel (Zhang and Xing 2007). Therefore, an obvious characteristic of the continuous-flow PCR is that the cycling rates of PCR amplification can be adjusted by changing the velocities of the PCR solution through the reaction channel. Figure 3 shows the online fluorescence detection and AGE results of the nested PCR products generated at flow velocities of 2, 3.5, 5, 7.5 and 10 mm/s (Fig. S4). The product from the conventional thermal cycler was used as a reference to understand the biochemical performance in amplification efficiency at different flow velocities. The results from Fig. 3 clearly show that within the first and second SP-CF-PCR runs, the yields of PCR amplification are gradually reduced with the increase of flow rates in the microchannel, but the PCR speed is increased gradually. This is primarily attributed to the fact that for the CF-PCR microfluidics, the small thermal inertia, only from the PCR mixture rather than entire reactor, enables only the sample flow rate and the time to reach thermal equilibrium to determine the temperature transition. As the flow rate increased, the available time for the reaction solution to reach thermal equilibrium and/or keep at set-point temperature was reduced, and thus the amount of PCR product was decreased (Hashimoto et al. 2004). At the flow rate of 2 mm/s, the amount of the second-run PCR product is approximately equal to that of the first continuous-flow PCR run ("2" column in Fig. 3a; lane 1 of Fig. 3b, c). When the flow rates were raised up to 5 mm/s, the gel images of the first and second PCR products were still very clear, indicating the two successful amplifications were obtained (lane 3 in Fig. 3b, **c**). With increasing the flow rates to 7.5 and 10 mm/s, the corresponding electrophoresis results was hardly distinguished (lanes 4 and 5 in Fig. 3b, c), but the online fluorescence detection result in the case of 7.5 mm/s can be still screened out, further indicating that the online fluorescence detection method is more sensitive than the AGE analysis. The above experimental results further show that the

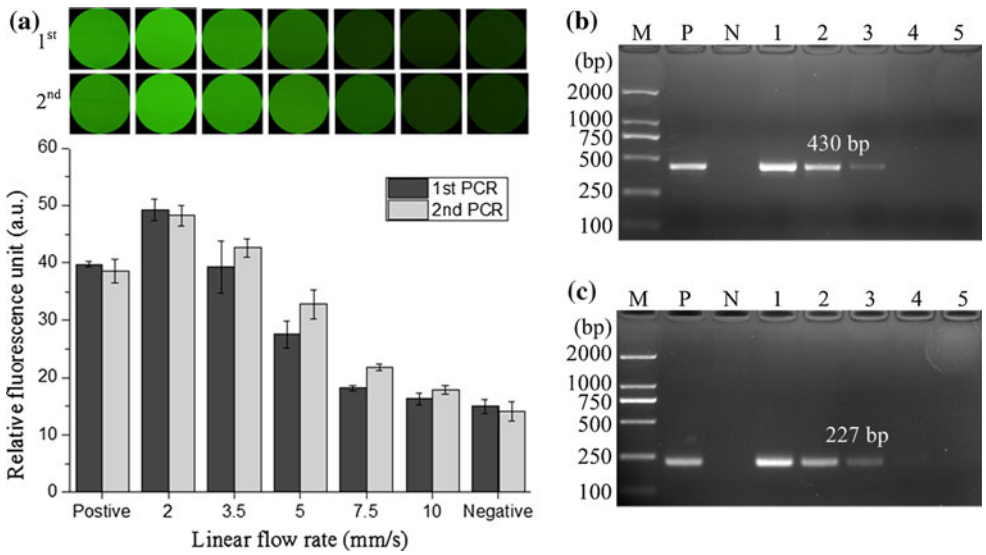

Fig. 3 Effect of flow rates on SP-CF-NPCR. **a** Fluorescence detection of the SP-CF-NPCR products. Here, the *error bars* represent the standard deviation of the average values of three individual experiments. **b** Gel analysis of the first-run PCR products. *Lane P* the positive control PCR product from the conventional PCR machine. *Lane N* the negative-control PCR with no template on the SP-CF-NPCR at 2 mm/s. *Lane 1–5* the first-run products from SP-CF-NPCR at 2, 3.5, 5, 7.5 and 10 mm/s (2 μL DNA template of 2.5×10^5 copies/μL). **c** Gel analysis of the second-run products. *Lane P* the positive control PCR product from the conventional PCR machine. *Lane N* the negative-control PCR with no template on the SP-CF-NPCR device at 2 mm/s. *Lane 1–5* the second-run products from the SP-CF-NPCR at 2, 3.5, 5, 7.5, and 10 mm/s. Here, 2-μL first-run PCR product that was diluted 400-fold with DNA-free water was used as second-run PCR templates

presented SP-CF-NPCR reaction can be accomplished between 18 and 50 min (at flow rates of 2 and 7.5 mm/s, the amplification times were 25 min and 9 min, respectively). It should be noted that the no-template controls performed on the CF-PCR microfluidic device with all assay reagents and ddH_2O instead of DNA template also showed a weak fluorescence signal which probably came from unspecific SYBR Green I binding to the primer-dimers (Cady et al. 2005). Considering that there is a trade-off between rapidness and PCR yield due to the limited extension rate of Taq DNA polymerase and thermal inertial effects (Hashimoto et al. 2004; Crews et al. 2008), and that the focus of the present study lies in highly sensitive detection of minute amounts of pathogenic bacteria, the linear flow rate of 2 mm/s for the first CF-PCR run and 3.5 mm/s for the second CF-PCR run are utilized within the following test of limit of detection (LOD).

3.4 Effect of the amount of input DNA molecules on single-phase continuous-flow nested PCR

For clinical applications such as detection of foodborne pathogens, it is essential to obtain a detectable amount of amplification product quickly from a low-abundance sample. Therefore, it is necessary to investigate the correlation between the amount of SP-CF-NPCR products and the concentrations of initial DNA sample on the presented device. Here, tenfold serial dilutions of genomic DNA from *L. monocytogenes* ranging from 2.5×10^5 to 2.5 copies/μL were prepared as PCR templates to determine the LOD. Figure 4a shows the online fluorescence detection results of SP-CF-NPCR from the serially diluted *L. monocytogenes* DNA (Fig. S5a). Figure 4b and c shows the corresponding AGE results (Fig. S5b and c). As seen from Fig. 4, the yields of first-run CF-PCR products were reduced with the decrease of the concentration of the initial DNA samples, and the second CF-PCR run displayed a similar trend. When the initial DNA samples of higher concentrations (2.0×10^3 or 2.0×10^4 copies/μL) were used, the first and second CF-PCR runs obtained successful target amplifications, but there were the obvious bands of 430-bp and 273-bp PCR products in the second PCR run (lanes 1 and 2 in Fig. 4b, c). This phenomenon is mainly attributed to the fact that in the first CF-PCR run the initial template of higher concentration resulted in more amplification products those were further used as the template of the second CF-PCR run. The second-run CF-PCR products using DNA templates of higher concentrations have been sequenced, and the sequencing results demonstrated that the 273-bp PCR product was produced by the forward primer of the outer product and the reverse primer of the inner product (Fig. S6b and d) and that the 227-bp and 430-bp PCR products were the second-run and first-run amplification of interest (Fig. S6a, c and e). It is to note that the melting curve analysis (MCA) can be relatively easily integrated on the presented device to identify these fluorescence products (Pjescic and Crews 2012). In addition, it needs to point out that the fluorescence signal was not proportional to the amount of 227-bp product when the

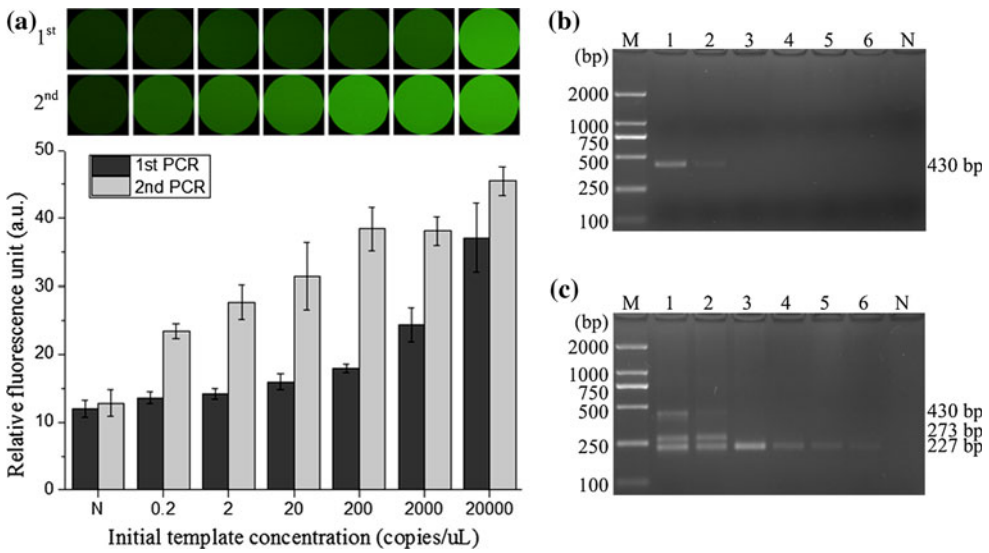

Fig. 4 Effect of amount of input DNA on SP-CF-NPCR. **a** Fluorescence detection of the SP-CF-NPCR products. Here, the *error bars* represent the standard deviation of the average values of three individual experiments. **b** Gel analysis of the first-run PCR products. *Lane M* Marker. *Lane 1–6* the first-run products from tenfold serial dilution of *L. monocytogenes* genomic DNA that was estimated from 2.0×10^4 to 2.0×10^{-1} copies/μL. *Lane N* the negative-control PCR with no template on the SP-CF-NPCR at 2 mm/s. **c** Gel analysis of the second-run PCR products. *Lane N* the negative-control PCR on the SP-CF-NPCR at 3.5 mm/s. *Lane 1–6* the second-run products using 2 μL of the first-run products in (**b**) as templates

templates of high concentrations were used ("2000" and "20000" columns in Fig. 4a). Thus, the presented fluorescence detection method is not reliable for quantitative measurement of the SP-CF-NPCR products. With decreasing the concentrations of the initial DNA samples, the bands of 430-bp and 273-bp PCR products in the second PCR run could not be detected on the gel electrophoretic image, but the 227-bp target fragment of amplification could be detected well (lanes 3–6 in Fig. 4b, c). For the presented SP-CF NPCR, the lowest concentration of the initial template at which positive fluorescence signal could be detected was 0.2 copies/μL or 5 copies per reaction ("0.2" column in Fig. 4a; lane 6 in Fig. 4c). To further confirm this sensitivity of the presented SP-CF NPCR assay, ten replicates were performed and the results are shown in Fig. S7 and the related discussion can be found in ESM. To the best of our knowledge, this is the most sensitive single-phase continuous-flow PCR microsystem reported in the literature. This sensitivity is mainly attributed to the implementation of the nested PCR protocol in the presented single-phase continuous-flow PCR microsystem. In addition, the combination of static and dynamic inner surface passivation used in this work may help improve the detection sensitivity. When compared to the conventional PCR assays for *Listeria* detection, the presented SP-CF NPCR assay can obtain the comparable detection sensitivity in a shorter time (Table S1 and its related discussion in ESM). In addition, compared with other some microfluidic PCR devices exhibiting relatively high sensitivity (Chen et al. 2007; Wang and Burns 2010; Lok et al. 2012), the presented SP-CF-NPCR microfluidic platform has some obvious advantages: (1) flexible reaction volumes. Assay volumes ranging from several microliters to 100 μl or even higher can be adopted if required, due to the inherent nature of the presented single-phase continuous-flow PCR system's structural and fluidic design. Therefore, this system provides a promising solution for ensuring statistical confidence with a relatively large volume to contain enough of the target molecules in case of target analytes present at low concentrations; (2) convenience of continuous operation. The reaction mixture unidirectionally flows through the single capillary microchannel to complete the biochemical reactions, enabling a convenient fluid manipulation for the continuous multi-step process without valves or other sealing approaches (Chen et al. 2005a, b; Pjescic and Crews 2012).

3.5 Detection of unpurified DNA or clinical samples on single-phase continuous-flow nested PCR

It is true that the purified and highly concentrated DNA samples are often used to evaluate the new continuous-flow PCR technology, and the additional pre-processing of samples for successful PCR amplifications is required. For practical applications such as clinical diagnosis, however, it is essential to determine the presence of target molecules from unpurified DNA or unprocessed clinical samples. To investigate the possibility of practical application of the presented SP-CF-NPCR technology, the unpurified DNA

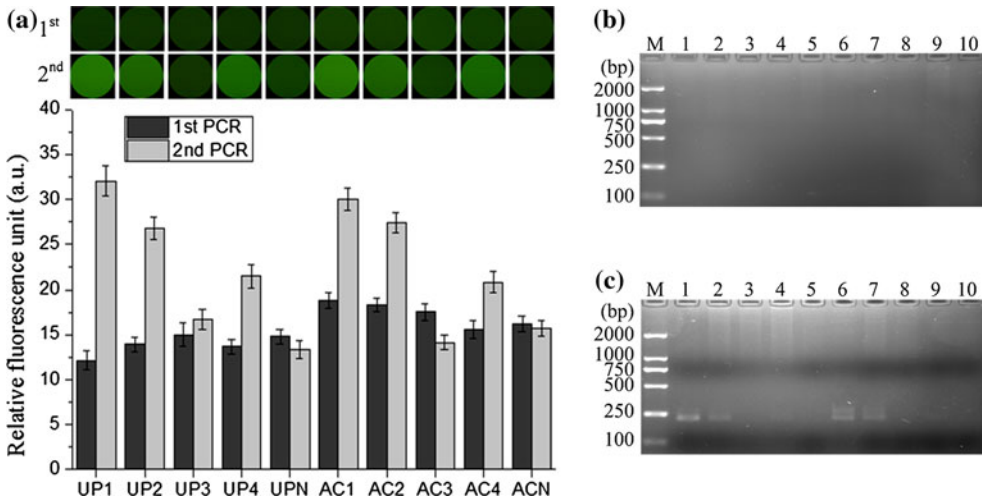

Fig. 5 Detection of unpurified DNA and artificially clinical samples on the SP-CF-NPCR device. **a** Fluorescence detection of the SP-CF-NPCR products from unpurified DNA samples (UP) and artificially clinical samples (AC). UP1-UP3: thermally lysed bacterial cells of 2.0×10^5, 2.0×10^4, 2.0×10^3 CFU mL^{-1} (2 μL); UP4: thermally lysed bacterial cells of 2.0×10^3 CFU mL^{-1} (5 μL); UPN: the negative control with no bacterial cells (2 μL); AC1-AC3: DNA isolated from stool samples with bacterial cells of 1.0×10^6, 1.0×10^5, 1.0×10^4 CFU mL^{-1} (2 μL); AC4: tenfold diluted DNA from stool samples with bacterial cells of 1.0×10^5 CFU mL^{-1} (2 μL); ACN: the negative control of stool DNA samples without bacterial cells (2 μL); **b** Gel analysis of the first-run PCR products. *Lane M* Marker; *Lane 1–5* correspond to UP1-UP5 in the (**a**) panel; *Lanes 6–10* correspond to AC1-AC5 in the (**a**) panel. **c** Gel analysis of the second-run PCR products. *Lane M* Marker. *Lane 1–10* the second-run products using 2 μL of the first-run products in (**b**) as templates

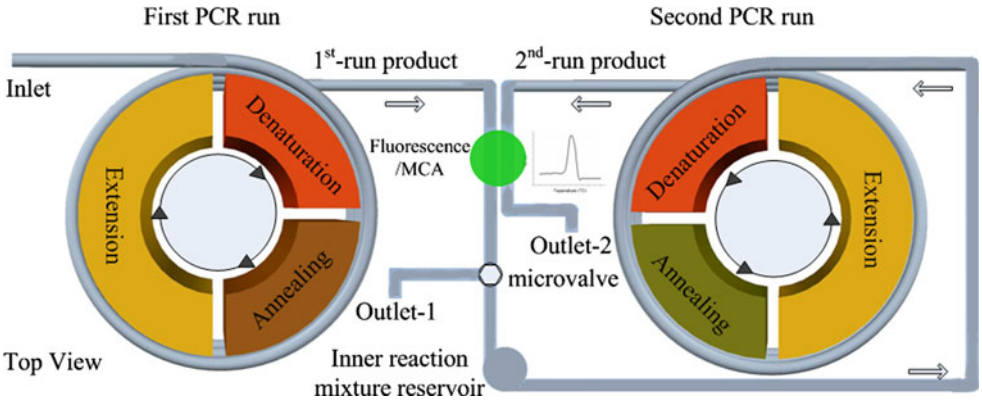

Fig. 6 Schematic of the automated SP-CF-NPCR microsystem

samples and artificially clinical samples were tested. Briefly, the cultured bacterial cells were thermally lysed and used for the unpurified DNA samples, while the artificially clinical samples were the health human stool contaminated with bacterial cells and the DNAs were isolated using the DNA purification Kit. The detailed sample preparation procedures can be found in the ESM. Figure 5a shows the fluorescence detection results of the SP-CF-NPCR products using unpurified DNA samples and artificially clinical samples. Figure 5b and c display the corresponding gel electrophoresis results. As seen from Fig. 5a, b, using the unpurified DNA samples or the DNAs isolated from the artificially clinical samples, no positive fluorescence signals or bands could be observed after the first run of the SP-CF-NPCR, as similar to the results using the purified DNA samples with low template numbers. However, the second-run PCR could generate obvious amplification products using the relatively high bacterial cell numbers (columns UP1, UP2 and AC1, AC2 in Fig. 5a; lanes 1, 2 and 6, 7 in Fig. 5c). In the case of the low bacterial cell numbers, the second-run PCR did not produce detectable amplification products (columns UP3 and AC3 in Fig. 5a; lanes 3 and 8 in Fig. 5c). The possible explanations are that the low cell numbers were used (for the UP3 case) and the presence of PCR inhibitor(s) (since the stool specimens are highly complex and contain diverse inhibitory materials) (for the AC3 case). These explanations are probably demonstrated by the experiments in the UP4 and AC4 cases, where the volume of the template sample in the UP4 case was 2.5 times of that in the UP3 case and the input DNA samples used in the AC4 case was tenfold diluted from those used in the AC2 case (columns UP4 and AC4 in Fig. 5a; lanes 4 and 9 in Fig. 5c). Here, it is necessary to note that the SP-CF NPCR technology was capable of detecting as few as 10 cells/reaction in the case of unpurified DNA ("UP4" column in Fig. 5a; lane 4 in Fig. 5c) and about 100 cells/reaction for the artificially contaminated clinical samples ("AC2" column in Fig. 5a; lane 7 in Fig. 5c), assuming a 100 % DNA recovery from the bacterial cell samples.

3.6 Future development of automated single-phase continuous-flow nested PCR microsystem

The nested PCR approach based on single-phase continuous-flow strategy proposed here also offers the possibility of using microfluidic technology to automatically perform a nested PCR reaction without any risk of cross-contamination. The end-point fluorescent detection or MCA-based product identification method can be integrated onto the microfluidic device for online detection of the first-run and second-run PCR products (Fig. 6). This automation operating scheme combined with the high sensitivity of the device allows for rapid and sensitive target DNA detection with no risk for cross-contamination. Here, it needs to be noted that for the nested PCR quantifying the copy number of the template is often quite difficult and not very accurate. Fortunately, however, real-time quantitative PCR can be realized in this microfluidic PCR format (Park et al. 2003; Nakayama et al. 2006). Park et al. (2003) for the first time developed the cylindrical compact continuous-flow PCR device and proposed the real-time PCR to be easily realized in their continuous-flow technique. Since there is an air gap between the extension and denaturing blocks, the parallel, bridging parts of the capillary can be severed as windows of quantitative fluorescence detection during amplification. A TaqMan-based quantitative continuous-flow PCR was developed on the polydimethylsiloxane (PDMS)/glass hybrid chip device (Nakayama et al. 2006). In our future real-time SP-CF-NPCR device, the fluorescence artifacts caused by incorrect amplification products could be effectively avoided by using sequence-specific labeled probes or Taqman/molecular beacons instead of SYBR Green I. And, the real-time SP-CF-NPCR in this model can be used to quantify the copy number of the template in the original sample.

4 Conclusion

In summary, we have developed a SP-CF-NPCR microfluidics for highly sensitive detection of foodborne

pathogens. *L. monocytogenes*, an important foodborne pathogen, was used to evaluate the microfluidic method described here. Using the presented system, the minute amount of genomic DNA from this organism could be successful amplified and detected. The effects of reaction parameters, such as polymerase concentration, linear flow rates and template DNA concentration on the performance of SP-CF-NPCR have been experimentally evaluated. The experimental results showed that, the sensitivity of detection was high up to 0.2 copies/μL and the detection could be completed in 42 min. In addition, the results of our study also indicate that it will be possible to develop the SP-CF-NPCR at the single-molecule level for detection of foodborne pathogens. If successfully developed, the presented highly sensitive method would find applications in more areas (Zhang and Xing 2010). Finally, it should be noted that the on-line fluorescence detection method described here is only a qualitative or semi-quantitative detection approach that seems to be inadequate for a quantitative measurement of the amplified products, which may be overcome by the real-time quantitative or MCA method integrated on the SP-CF-NPCR device.

Acknowledgments This research is supported by the National Natural Science Foundation of China (61072030), the National Basic Research Program of China (2010CB732602), the Key Program of NSFC-Guangdong Joint Funds of China (U0931005), and the Program for Changjiang Scholars and Innovative Research Team in University (IRT0829).

References

Anderson RC, Su X, Bogdan GJ, Fenton J (2000) A miniature integrated device for automated multistep genetic assays. Nucleic Acids Res 28(12):e60

Batt CA (2007) Materials science—food pathogen detection. Science 316(5831):1579–1580

Beyor N, Yi L, Seo TS, Mathies RA (2009) Integrated capture, concentration, polymerase chain reaction, and capillary electrophoretic analysis of pathogens on a chip. Anal Chem 81(9):3523–3528

Cady NC, Stelick S, Kunnavakkam MV, Batt CA (2005) Real-time PCR detection of *Listeria monocytogenes* using an integrated microfluidics platform. Sens Actuat B 107(1):332–341

Chen ZY, Qian SZ, Abrams WR, Malamud D, Bau HH (2004) Thermosiphon-based PCR reactor: experiment and modeling. Anal Chem 76(13):3707–3715

Chen JF, Wabuyele M, Chen HW, Patterson D, Hupert M, Shadpour H, Nikitopoulos D, Soper SA (2005a) Electrokinetically synchronized polymerase chain reaction microchip fabricated in polycarbonate. Anal Chem 77(2):658–666

Chen ZY, Wang J, Qian SZ, Bau HH (2005b) Thermally-actuated, phase change flow control for microfluidic systems. Lab Chip 5(11):1277–1285

Chen L, West J, Auroux PA, Manz A, Day PJR (2007) Ultrasensitive PCR and real-time detection from human genomic samples using a bidirectional flow microreactor. Anal Chem 79(23):9185–9190

Crabtree HJ, Lauzon J, Morrissey YC, Taylor BJ, Liang T, Johnstone RW, Stickel AJ, Manage DP, Atrazhev A, Backhouse CJ, Pilarski LM (2012) Inhibition of on-chip PCR using PDMS-glass hybrid microfluidic chips. Microfluid Nanofluid 13(3):383–398

Crews N, Wittwer C, Gale B (2008) Continuous-flow thermal gradient PCR. Biomed Microdevices 10(2):187–195

Hashimoto M, Chen PC, Mitchell MW, Nikitopoulos DE, Soper SA, Murphy MC (2004) Rapid PCR in a continuous flow device. Lab Chip 4(6):638–645

Hua Z, Rouse JL, Eckhardt AE, Srinivasan V, Pamula VK, Schell WA, Benton JL, Mitchell TG, Pollack MG (2010) Multiplexed real-time polymerase chain reaction on a digital microfluidic platform. Anal Chem 82(6):2310–2316

Kopp MU, de Mello AJ, Manz A (1998) Chemicalf amplification: continuous-flow PCR on a chip. Science 280(5366):1046–1048

Li YY, Zhang CS, Xing D (2011a) Integrated microfluidic reverse transcription-polymerase chain reaction for rapid detection of food- or waterborne pathogenic rotavirus. Anal Biochem 415(2):87–96

Li YY, Zhang CS, Xing D (2011b) Fast identification of foodborne pathogenic viruses using continuous-flow reverse transcription-PCR with fluorescence detection. Microfluid Nanofluid 10(2):367–380

Liu RH, Yang JN, Lenigk R, Bonanno J, Grodzinski P (2004) Self-contained, fully integrated biochip for sample preparation, polymerase chain reaction amplification, and DNA microarray detection. Anal Chem 76(7):1824–1831

Liu HB, Ramalingam N, Jiang Y, Dai CC, Hui KM, Gong HQ (2009) Rapid distribution of a liquid column into a matrix of nanoliter wells for parallel real-time quantitative PCR. Sens Actuat B 135(2):671–677

Lok KS, Lee PPF, Kwok YC, Nam-Trung N (2012) Nested PCR in magnetically actuated circular closed-loop PCR microchip system. Microchim Acta 177(1–2):111–117

Manage DP, Morrissey YC, Stickel AJ, Lauzon J, Atrazhev A, Acker JP, Pilarski LM (2011) On-chip PCR amplification of genomic and viral templates in unprocessed whole blood. Microfluid Nanofluid 10(3):697–702

Nakayama T, Kurosawa Y, Furui S, Kerman K, Kobayashi M, Rao SR, Yonezawa Y, Nakano K, Hino A, Yamamura S, Takamura Y, Tamiya E (2006) Circumventing air bubbles in microfluidic systems and quantitative continuous-flow PCR applications. Anal Bioanal Chem 386(5):1327–1333

Njoroge SK, Witek MA, Battle KN, Immethun VE, Hupert ML, Soper SA (2011) Integrated continuous flow polymerase chain reaction and micro-capillary electrophoresis system with bioaffinity preconcentration. Electrophoresis 32(22):3221–3232

Northrup MA, Ching MT, White RM, Watson RT (1993) DNA amplification in a microfabricated reaction chamber. In: Proceeding of the 7th international conference on solid state sensors and actuators, Yokohama, Japan, pp 924–926

Park N, Kim S, Hahn JH (2003) Cylindrical compact thermal-cycling device for continuous-flow polymerase chain reaction. Anal Chem 75(21):6029–6033

Park S, Zhang Y, Lin S, Wang TH, Yang S (2011) Advances in microfluidic PCR for point-of-care infectious disease diagnostics. Biotechnol Adv 29(6):830–839

Peham JR, Grienauer W, Steiner H, Heer R, Vellekoop MJ, Noehammer C, Wiesinger-Mayr H (2011) Long target droplet polymerase chain reaction with a microfluidic device for high-throughput detection of pathogenic bacteria at clinical sensitivity. Biomed Microdevices 13(3):463–473

Pjescic I, Crews N (2012) Genotyping from saliva with a one-step microdevice. Lab Chip 12(14):2514–2519

Polini A, Mele E, Sciancalepore AG, Girardo S, Biasco A, Camposeo A, Cingolani R, Weitz DA, Pisignano D (2010) Reduction of

water evaporation in polymerase chain reaction microfluidic devices based on oscillating-flow. Biomicrofluidics 4(3):036502
Prakash AR, Amrein M, Kaler KVIS (2008) Characteristics and impact of Taq enzyme adsorption on surfaces in microfluidic devices. Microfluid Nanofluid 4(4):295–305
Qiu X, Mauk MG, Chen D, Liu C, Bau HH (2010) A large volume, portable, real-time PCR reactor. Lab Chip 10(22):3170–3177
Qiu X, Chen D, Liu C, Mauk MG, Kientz T, Bau HH (2011) A portable, integrated analyzer for microfluidic-based molecular analysis. Biomed Microdevices 13(5):809–817
Ramalingam N, Liu HB, Dai CC, Jiang Y, Wang H, Wang Q, Hui MK, Gong HQ (2009) Real-time PCR array chip with capillary-driven sample loading and reactor sealing for point-of-care applications. Biomed Microdevices 11(5):1007–1020
Ramalingam N, Rui Z, Liu HB, Dai CC, Kaushik R, Ratnaharika B, Gong HQ (2010) Real-time PCR-based microfluidic array chip for simultaneous detection of multiple waterborne pathogens. Sens Actuat B 145(1):543–552
Ritzi-Lehnert M, Himmelreich R, Attig H, Claussen J, Dahlke R, Grosshauser G, Holzer E, Jeziorski M, Schaeffer E, Wende A, Werner S, Wiborg JO, Wick I, Drese KS, Rothmann T (2011) On-chip analysis of respiratory viruses from nasopharyngeal samples. Biomed Microdevices 13(5):819–827
Schaerli Y, Hollfelder F (2009) The potential of microfluidic water-in-oil droplets in experimental biology. Mol BioSyst 5(12): 1392–1404
Sciancalepore AG, Polini A, Mele E, Girardo S, Cingolani R, Pisignano D (2011) Rapid nested-PCR for tyrosinase gene detection on chip. Biosens Bioelectron 26(5):2711–2715
Shi X, Lin LI, Chen SY, Chao SH, Zhang WW, Meldrum DR (2011) Real-time PCR of single bacterial cells on an array of adhering droplets. Lab Chip 11(13):2276–2281
Sun Y, Dhumpa R, Bang DD, Hogberg J, Handberg K, Wolff A (2011a) A lab-on-a-chip device for rapid identification of avian influenza viral RNA by solid-phase PCR. Lab Chip 11(8):1457–1463
Sun Y, Dhumpa R, Bang DD, Handberg K, Wolff A (2011b) DNA microarray-based solid-phase RT-PCR for rapid detection and identification of influenza virus type A and subtypes H5 and H7. Diagn Microbiol Infect Dis 69(4):432–439
Wang F, Burns MA (2009) Performance of nanoliter-sized droplet-based microfluidic PCR. Biomed Microdevices 11(5):1071–1080
Wang F, Burns MA (2010) Droplet-based microsystem for multi-step bioreactions. Biomed Microdevices 12(3):533–541
Yang JN, Liu YJ, Rauch CB, Stevens RL, Liu RH, Lenigk R, Grodzinski P (2002) High sensitivity PCR assay in plastic micro reactors. Lab Chip 2(4):179–187
Zeng Y, Novak R, Shuga J, Smith MT, Mathies RA (2010) High-performance single cell genetic analysis using microfluidic emulsion generator arrays. Anal Chem 82(8):3183–3190
Zhang CS, Xing D (2007) Miniaturized PCR chips for nucleic acid amplification and analysis: latest advances and future trends. Nucleic Acids Res 35(13):4223–4237
Zhang CS, Xing D (2009) Parallel DNA amplification by convective polymerase chain reaction with various annealing temperatures on a thermal gradient device. Anal Biochem 387(1):102–112
Zhang CS, Xing D (2010) Single-molecule DNA amplification and analysis using microfluidics. Chem Rev 110(8):4910–4947